

Automatic Segmentation Methodology for Dermatological Images Acquired via Mobile Devices

Luís Rosado and Maria João M. Vasconcelos

Fraunhofer Portugal AICOS, Porto, Portugal

Keywords: Mobile Devices, Segmentation, Teledermatology.

Abstract: Nowadays, skin cancer is considered one of the most common malignancies in the Caucasian population, thus it is crucial to develop methodologies to prevent it. Because of that, Mobile Teledermatology (MT) is thriving, allowing patients to adopt an active role in their health status while facilitating doctors to early diagnose skin cancers. Skin lesion segmentation is one of the most important and difficult task in computerized image analysis process, and so far the attention is mainly turned to dermoscopic images. In order to turn MT more accurate, it is therefore fundamental to develop simple segmentation methodologies specifically designed for macroscopic images or images acquired via smartphones, which is the main focus of this work. The proposed method was applied in 80 images acquired via smartphones and promising results have been achieved: a mean Jaccard index of 81%, mean True Detection Rate of 96% and mean Accuracy around 98%. The major goal of this work is to develop a mobile application easily accessible for the general population, with the aim of raise awareness and help both patients and doctors in the early diagnosis of skin cancers.

1 INTRODUCTION

The early detection of malignant skin lesions is fundamental for a successful treatment. The melanoma-based mortality rates are as high as 23%, where the majority are due to missed or late diagnosed melanomas. In this context, Mobile Teledermatology has the potential to improve efficiency and quality aspects of care at lower costs and empowers patients to adopt an active role in managing their own health status while facilitating the early diagnosis of skin cancers.

Segmentation of skin lesions is one of the most important and difficult task in computerized image analysis process and its success considerably influences the accuracy of the subsequent steps. However, up until now the majority of the available skin lesion segmentation methods are optimal for dermoscopic images. While for dermatological or macroscopic images, like images obtained by mobile phones or cameras, there is still the need to evolve on the development of methods for segmenting this type of images. The present study investigates the acquisition and segmentation of skin lesion images acquired via mobile devices.

Considering that a pigmented skin lesion is a depigmentation of the skin, many of the segmen-

tation methods start by converting the input image from color to grayscale and try to distinguish between skin mole and surrounding skin pixels. Several methods have been proposed for the segmentation of dermoscopic images. The Otsu's thresholding method (Otsu, 1979) has been widely used for this purpose (Manousaki et al., 2006; Tabatabaie et al., 2009). Later, (Cavalcanti et al., 2010) employed Otsu's method only in the Red channel from the RGB color space obtaining good segmentation results. Other researchers proposed to use Snakes (or Active-Contours) for skin lesion segmentation, like in (Mahmoud and Al-Jumaily, 2011) that the authors also use the grayscale image, apply Wiener and Median filters to remove noise and hairs, threshold the filtered image and propose a Gradient Vector Flow snake to obtain the final contour, or as in (Ivanovici and Stoica, 2012) where a multiscale approach for active contours is proposed for color images. Oppositely, (Cavalcanti et al., 2011) observed that when independent component analysis (ICA) is applied to the image, one of the resultant ICA component corresponds mainly to the lesion area and proposed determining the lesion boundary more precisely using the Chan-Vese Active contours method.

The rest of the paper is organized as follows: In section 2, the dataset used in the study is presented as

well as the mobile application developed to obtain the best possible quality images during the image acquisition process. Our proposed segmentation methodology for dermatological images acquired via mobile devices is described in section 3. Section 4 presents and discusses the obtained results. Finally, in section 5 conclusions are made and future directions drawn.

2 DATASET

Our study intends to assess the segmentation quality of dermatological images acquired with a smartphone. Based on what is known, there is no publicly available image database that includes dermatological images with the ground truth for segmentation. So we have used the database collected at the Portuguese Institute of Oncology of Porto (IPO), under the scope of the project Melanoma Detection (Fraunhofer, 2014). The images were acquired during 4 appointments with 2 dermatologists, where the project was previously explained to the patients and the statement of agreement obtained. The database contains a total of 80 images, corresponding to 80 different skin moles, obtained from 31 subjects (14 males and 17 females) with ages between 28 and 70 years (mean age around 43 years). They are 24-bit color images with 652x652 pixels of resolution, acquired with a mobile phone HTC One S.

With the purpose of helping the image acquisition process of the referred dataset, a mobile application was developed for the Android OS that performs real-time detection of the square region of interest of the target skin lesion. As shown in Figure 1.a, the user must place the circular red target located at the center of the screen inside the skin lesion. Only when the skin lesion is detected, the circular target becomes green (see Figure 1.a and 1.b) and the application allows to acquire a image with the maximum resolution supported by the smartphone. Since this process guarantees that the skin lesion is at the center of the circular target, the acquired image at maximum resolution is then cropped to the black square shown on Figure 1.a, being this the square region of interest image of the target skin lesion (see Figure 1.c). It is worth noting that the real-time skin lesion detection uses a preview image with a significantly lower resolution when compared with the acquired image, in order to decrease processing time per frame. With the HTC One S smartphone, the preview image has a resolution of 960x544 pixels (Figure 1.a and 1.b), the acquired image has 3264x1840 pixels, while the resulting square region of interest is an image of 652x652 pixels (Figure 1.c). The resolution of this last image is

imposed by the minimum focus distance of the camera (around 5.5 cm for HTC One S), which guarantees the maximum resolution for the skin mole image.

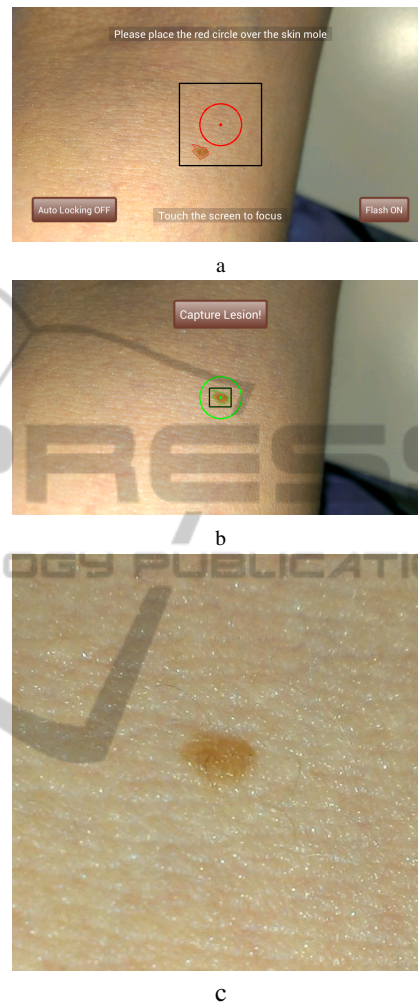


Figure 1: Android application screenshots of: (a) skin lesion not detected; (b) skin lesion detected, which allows the image acquisition at maximum resolution; (c) Square region of interest image acquired at maximum resolution.

The real-time detection of the skin lesion on the preview images uses the same segmentation methodology that is later applied to the acquired square region of interest image (described in the following section). Furthermore, the developed mobile application respected the image acquisition protocol proposed on (Rosado et al., 2012):

1. The smartphone camera should be kept directly perpendicular to the target skin area during the image acquisition.
2. The smartphone camera should be at the minimum focus distance from the skin mole, in order to ensure maximum image resolution.



Figure 2: Examples of original images (first row) and manual border from two the authors (border contour in white).

3. The smartphone intrinsic flash light should be used in the image acquisition.
4. The autofocus should be used in the image acquisition process. In particular, the macro focus mode should be used if available, and the skin lesion must be in the center of the image to ensure a better automatic focusing.

The IPO Mobile dataset was then acquired using the described mobile application, and each acquired image was later manually segmented by the authors, generating two different ground truth datasets (see Figure 2).

3 SEGMENTATION METHODOLOGY

The proposed methodology comprises six main blocks, as shown in Figure 3.

The original image is firstly transformed Red-Green-Blue image (RGB) into a grayscale image and

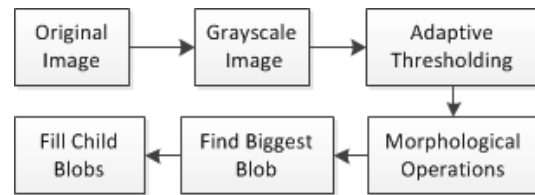


Figure 3: Block diagram for the segmentation methodology of skin lesion images acquired via mobile devices.

an adaptive thresholding is applied, as explained next.

Considering an original image I_L , the corresponding segmented I_S obtained by adaptive thresholding is given by the following equation:

$$I_S(x,y) = \begin{cases} 0 & \text{if } I_L(x,y) > T_L(x,y) \\ 255 & \text{otherwise} \end{cases} \quad (1)$$

where T_L is the mean intensity value of the square region centered on the pixel location (x,y) with a side value of R_S minus the constant C . In the proposed approach, it is used $C=10$, defined empirically, and:

$$R_S = \frac{\max\{Image_{width}, Image_{height}\}}{2} \quad (2)$$

Afterwards, a sequence of three opening morphological operations (erosion followed by dilatation) is applied to the binary image with the purpose of smoothing the object contours, eliminating narrow extensions and breaking thin connections between the objects. The subsequent step consists on finding the largest object in the segmented image and consider it as the region that represents the skin lesion, being all the other regions discarded. Since the detection of the biggest blob demands comparing all objects areas in the image, a median filter is previously applied to eliminate small objects, thus, significantly decreasing the processing time of this step. At last, all the holes inside the selected object are filled, and the final segmented image is obtained.

4 RESULTS

As previously referred, each image was manually segmented by the authors and two different ground truth datasets were generated. The suggested method was implemented in C++ and the average computational time for the segmentation at 134 milliseconds using an Intel® Core™2 Quad CPU Q9400 with 2.66GHz.

Figure 4 depicts some examples of the segmentation results obtained with our methodology overlapped with the ground truth datasets. From the images observation it can be seen that the proposed method achieves good segmentation results, with the

segmentation result being extremely close to both ground truth borders.

To quantify the discrepancy between manual and automatic segmentation, three distances were calculated: Jaccard index (J), True Detection Rate (TDR) and Accuracy.

The Jaccard index (Jaccard, 1912) is used to evaluate the overlap between the segmentation results and the ground truth:

$$J = \frac{\#(X \cap Y)}{\#(X \cup Y)}, \quad (3)$$

where X and Y are the binary representation of segmented object of the automatic method and the specialist, respectively and the operator # returns the number of pixels belonging to the object. This metric takes values between 0 and 1, where 1 corresponds to a perfect match between images and 0 when they are completely dissimilar.

The True Detection Rate (Silveira et al., 2009) is given by:

$$TDR = \frac{\#(X \cap Y)}{\#(Y)}. \quad (4)$$

While, Jaccard index and the TDR only consider the segmented regions, the Accuracy (Fraz et al., 2012) takes into consideration the whole image and is calculated by the formula:

$$Accuracy = \frac{\#(TN) + \#(TP)}{\#(TN) + \#(FP) + \#(FN) + \#(TP)}, \quad (5)$$

where TN is the number of true negative cases (number of pixels correctly classified as background), TP is the number of true positive cases (number of pixels correctly classified as object), FP is the number of false positive cases and FN is the number of false negative cases. An Accuracy of 1 means optimal segmentation.

For each segmentation image obtained through the proposed method, the Jaccard index, TDR and accuracy was calculated, taking into consideration both ground truth datasets separately. In addition, the Jaccard index between the ground truth datasets was also determined, with the purpose of comparing the discrepancy between the manual segmentations. Table 1 shows the resulting mean and standard deviation (std) values of the previously referred metrics. Analysing the results for the Jaccard index, the obtained mean error for the automatic segmentation was around 81% for both ground truth datasets (SvsG1 and SvsG2), and 88.36% for the comparison between the ground truth datasets (G1vsG2). This result (88.36%) indicates that exists a significant variability between the ground truth datasets, which should be taken into consideration when analyzing the error obtained for

Table 1: Jaccard, TDR and Accuracy mean and standard deviation values segmentation errors calculated for the 80 images - proposed method (S) and each ground truth dataset (G1, G2).

Jaccard (%)			
	SvsG1	SvsG2	G1vsG2
Mean	81.58	81.41	88.36
Std	8.68	8.10	4.73

TDR (%)			
	SvsG1	SvsG2	
Mean	97.38	95.56	
Std	3.93	6.14	

Accuracy (%)			
	SvsG1	SvsG2	
Mean	97.38	98.95	
Std	0.30	0.41	

the automatic segmentation (81%). The mean TDR around 97% and 96% with std of 4% and 6%, respectively, as well as the mean Accuracy of 97% and 99%, corroborate the results of the Jaccard index and confirms the quality of the present automatic segmentation methodology suggested.

Figure 5 presents the Jaccard distribution for the considered segmented images combinations, while Figures 6 and 7 present the TDR and accuracy distribution errors. It is possible to see that the referred metrics for the automated classification are not so different when comparing with both ground truth datasets separately. As expected, the distribution and mean error values are inferior for the combination that compares the ground truth datasets with each other. However, the results are only slightly worse, meaning that the automatic segmentation method performs well. Figures 6 and 7 show that TDR and Accuracy errors are very close to each other and with means near the optimal result (100%), where the worst (minimal values) are around 80% for TDR and 98% for Accuracy.

5 CONCLUSIONS AND FUTURE WORK

Most of available segmentation methods on the literature are directed to dermoscopic images. The need to promote the usage of Mobile Tele dermatology to facilitate the early diagnosis of skin cancers led us to explore and develop methodologies orientated to dermatological images acquired via mobile devices.

A mobile application for the Android OS was developed to help the image acquisition process, per-

forming real-time detection of the region of interest of the target skin lesion. In this work we also present a methodology to automatically segment skin lesions from dermatological images acquired via mobile devices. The method was applied in 80 smartphone-acquired images, achieving a mean Jaccard index result of 81%, mean True Detection Rate of 96% and mean Accuracy around 98%, confirming the adequacy of the suggested automatic segmentation methodology.

In order to expand this study in the near future, we consider that is important to have a testing dataset with more skin lesion images acquired via mobile devices, manually segmented by different specialists in the area and also investigate if the methodology is robust for different brands of mobile devices.

Above all, it is our goal to develop a mobile application easily accessible for the general population, with the aim of raise awareness and help both patients and doctors in the early diagnosis of skin cancers.

ACKNOWLEDGEMENTS

This work was done under the scope of the project “SMARTSKINS: A Novel Framework for Supervised Mobile Assessment and Risk Triage of Skin Lesion via Non-invasive Screening” with reference PTDC/BBB-BMD/3088/2012 financially supported by Fundação para a Ciência e a Tecnologia in Portugal.

REFERENCES

- Cavalcanti, P., Scharcanski, J., Di Persia, L., and Milone, D. (2011). An ICA-based method for the segmentation of pigmented skin lesions in macroscopic images. In *2011 Annual International Conference of the IEEE Engineering in Medicine and Biology Society, EMBC*, pages 5993–5996.
- Cavalcanti, P., Yari, Y., and Scharcanski, J. (2010). Pigmented skin lesion segmentation on macroscopic images. In *25th International Conference of Image and Vision Computing New Zealand*, pages 1–7.
- Fraunhofer, P. A. (2014). Melanoma detection, internal project. http://www.fraunhofer.pt/en/fraunhofer_aicos/projects/internal_research/melanoma_detection.html.
- Fraz, M. M., Remagnino, P., Hoppe, A., Uyyanonvara, B., Rudnicka, A. R., Owen, C. G., and Barman, S. A. (2012). Blood vessel segmentation methodologies in retinal images—a survey. *Computer methods and programs in biomedicine*, 108(1):407–433.
- Ivanovici, M. and Stoica, D. (2012). Color diffusion model for active contours—an application to skin lesion segmentation. In *2012 Annual International Conference of the IEEE, Engineering in Medicine and Biology Society (EMBC)*, pages 5347–5350. IEEE.
- Jaccard, P. (1912). The distribution of the flora in the alpine zone. 1. *New phytologist*, 11(2):37–50.
- Mahmoud, M. and Al-Jumaily, A. (2011). Segmentation of skin cancer images based on gradient vector flow (GVF) snake. In *2011 International Conference on Mechatronics and Automation (ICMA)*, pages 216–220.
- Manousaki, A. G., Manios, A. G., Tsompanaki, E. I., Panayiotides, J. G., Tsiftsis, D. D., Kostaki, A. K., and Tosca, A. D. (2006). A simple digital image processing system to aid in melanoma diagnosis in an everyday melanocytic skin lesion unit. a preliminary report. *International Journal of Dermatology*, 45(4):402–410.
- Otsu, N. (1979). A threshold selection method from gray-level histograms. *IEEE Transactions on Systems, Man and Cybernetics*, 9(1):62–66.
- Rosado, L., Castro, R., Ferreira, L., and Ferreira, M. (2012). Extraction of ABCD rule features from skin lesions images with smartphone. *Studies in health technology and informatics*, 177:242–247.
- Silveira, M., Nascimento, J. C., Marques, J. S., Marçal, A. R., Mendonça, T., Yamauchi, S., Maeda, J., and Rozeira, J. (2009). Comparison of segmentation methods for melanoma diagnosis in dermoscopy images. *IEEE Journal of Selected Topics in Signal Processing*, 3(1):35–45.
- Tabatabaie, K., Esteki, A., and Toossi, P. (2009). Extraction of skin lesion texture features based on independent component analysis. *Skin research and technology*, 15(4):433–439.

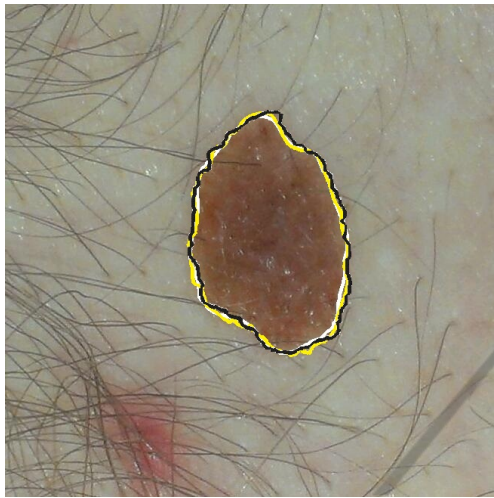


Figure 4: Examples of segmentation results: the ground truth borders are showed in white and yellow, while the border obtained using the proposed methodology appears in black, respectively.

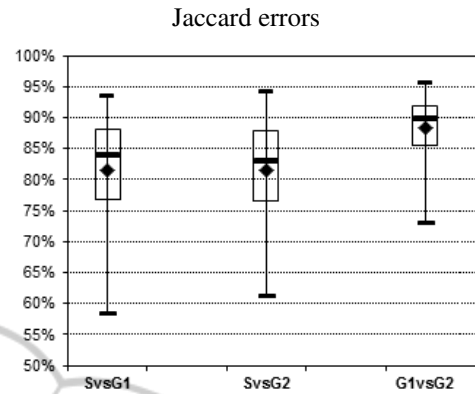


Figure 5: Jaccard distribution errors.

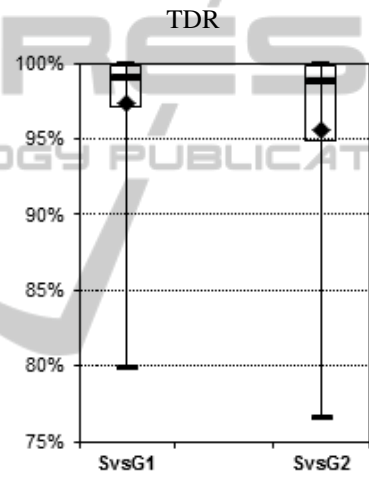


Figure 6: Distribution errors for True Detection Rate of the automated segmentation, considering the two ground truth datasets.

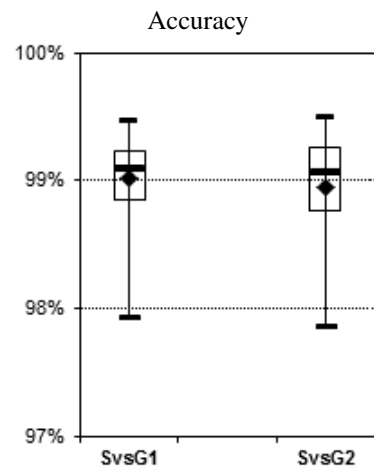


Figure 7: Distribution errors for Accuracy of the automated segmentation, considering the two ground truth datasets.